Crack tip analysis of a few transient loading situaitons at crack growth in stainless steel.

Ståhle, Per; Nilsson, Fred

1987

Document Version:
Förlagets slutgiltiga version

TEKNIKUM

UPPSALA UNIVERSITY
SCHOOL OF ENGINEERING
Department of Technology

UPTEC 87100 R

Date of issue
September 1987

Project name

Sponsoring organization
SKI

Author(s)

Per Ståhle and Fred Nilsson

Title (Swedish)

Title (English)

Crack tip analysis of a few transient loading situations at crack growth in stainless steel.

Abstract

The elasto plastic near tip field is examined for some different unloading-reloading situations. A linearly hardening material and a small scale of yielding is assumed.

By analytical estimation the regions of dominance for the asymptotic solutions for both the linearly hardening and the perfectly plastic material are obtained.

The experimental observations concerning crack growth rate after a sudden decrease in remote load as well as after an unloading-reloading cycle are explained.

Keywords / indexing

Security

Language
English

Supplementary bibliographical information

Pages
38

Classification

ISSN 0346-8887

ISBN

Postal address
Box 534
S-751 21 Uppsala
Sweden

Visiting address
Villavägen 4
Uppsala

Phone
+ 46-18-18 30 08 (librarian)
18 30 03 (office)

Telex
76143
UPTEC S

Crack tip analysis of a few transient loading situations at crack growth in stainless steel

It is here reported on a part of a larger finite element (FEM) investigation of fracture mechanical CERT-testing for corrosion fatigue under IGSCC conditions.

The rate of crack growth has in experiments been observed to drop significantly after an instantaneous but small decrease in remote load interrupting a steady state crack growth [1] (see Fig. 1). As the load later is recovered the rate of crack growth does not seem to be a unique function of remote load. After some amount of crack growth, of the order of the linear extension of the plastic zone the growth rate has assumed the level as observed at steady state, corresponding to the changed value of the loading.

Here the crack tip field is analysed as regards stresses and strains for a few different transient loads. At a FEM analysis a straight crack subjected to opening loads (mode I) is considered. The deformation is assumed to be plane. The linearly hardening material behaviour is governed by von Mises yield criterion and plastic flow is assumed to be associated to the yield criterion.

Applied load is the small scale yielding stress field given by

$$\sigma_{ij} = \frac{K_I}{\sqrt{2\pi r}} f_{ij}(\theta) \qquad \text{as} \quad r \to \infty \tag{1}$$

where $f_{ij}(\theta)$ are known functions.

The steady state problem is solved by employing a moving mesh technique. The solution obtained is valid also for the arrested crack. From this situation the load is a) decreased to 0.6 of full load, b) removed completely and then restored to 0.6 of full load, c) removed

completely and then fully restored . a), b) and c) are followed by crack growth simulated by a node relaxation technique. For reference, crack growth is simulated by node relaxation also immediately following the moving mesh solution without any interrupting changes in external load.

Steady state crack growth

Generally the transient crack growth, when starting from a virgin crack is rather small e.g. about two or three times the extension of the plastic zone. The initial transient crack growth is followed by a steady state crack growth that was reported on earlier [2].

Shortly after [2] was finished a solution [3] for the asymptotic near tip field for steady state crack growth in linearly hardening materials was reported. The analysis [3] follows the earlier attempt [4] to solve a similar crack growth problem but in [3] the analysis is improved while the possibility of a secondary plastic zone is considered. The result of [3] should therefore be more realistic since the presence of such a plastic zone is clearly indicated in numerical work (e.g. [2]). The final differential equations are solved by means of a Taylor's expansion in [4] whereas [3] formulates an eigen-value problem which is solved numerically by a Runge-Kutta technique.

The stress fields of the two investigations are essentially equal, at least in the regions above and ahead of the crack tip. As expected the deviation is large close to the crack surface because of the effects of reversed plasticity. Still deviations exposed when the results in [2] and [4] were compared, remain when the results of [2] now is compared with those of [3] (see Fig. 2). A much better coincidence is still achieved when [2] is compared with [5] in which analyses the near tip

field for a perfectly plastic material are made. This awakes the question of the range of validity for the solution [3] and [4] at the hardening rate considered.

The radial dependence of stresses was shown to be of r^s-type and the exponent s was calculated numerically in [3] and [4]. For a hardening rate $\alpha=0.01$ s was found to be 0.9113 but a best fit by application of the least square method acting on the FEM result [2] suggested a value $s=0.69$. In the latter case the crack surface displacements in the crack tip neighbourhood was utilized from a FEM solution for the complete small scale yielding problem (as opposed to the asymptotic analysis [4]). It was thus assumed that the numerical results [4] for s was erroneous possibly due to the neglected secondary plastic zone adjacent to the crack surface. Now as the result [3] which does include the secondary plastic zone in the analysis, is available showing that $s=0.9267$ for $\alpha=0.01$ which is not very far from the result of [4], it seems as if an explanation must be sought elsewhere.

The surprising similarities between the result [2] and the result for a perfectly plastic material [5] suggested an investigation from a new view point of an example provided by [3]. It can be shown for the anti-plane strain (mode III) case that two solutions exist for small values of α namely $r^{\sqrt{\alpha}}$ and $r^{-\sqrt{\alpha}}$. By chosing a model boundary value problem with reasonable boundary conditions remote from the crack tip in [3] it is shown that a two term solution approaches the result for a perfectly plastic material as the hardening rate α approaches zero. It is however rewarding to compare the two term solution for the displacement rate with the dominating-term approximation and secondly with the result for the perfectly plastic material. Thus

$$\dot{w}_{tt} = \dot{a}\,\frac{\tau_Y}{sG}\,[(r/R)^{-s} - (r/R)^{s}] \qquad (2)$$

is first compared with

$$\dot{w}_{st} = \dot{a} \frac{\tau_Y}{sG} (r/R)^{-s} \tag{3}$$

and secondly with

$$\dot{w}_{pp} = \dot{a} \frac{2\tau_Y}{G} \ln (R/r) \tag{4}$$

Here w is the out-of-plane displacement, a dot denotes time differentiation, G is the modulus of elasticity in shear, τ_Y is the shear yield stress, R is a length parameter of the order of the linear extension of the plastic zone and a is the crack growth rate. For s=0.1 the result is that w_{tt} (here assumed to be the exact solution) is approximated within 10% by w_{st} for

$$r < 10^{-5} R \tag{5}$$

Thus the approximation w_{st} is applicable in an extremely small region surrounding the crack tip. Unfortunately this region is as regards the investigated material surely much smaller than the fracture process region which at least is of the order of a grain in size. Note that a necessary condition when employing the asymptotic field in the analysis is that the field completely embeds the process region.

On the other hand w_{tt} is approximated (within 10%) by the solution for the perfectly plastic material w_{pp} within the range

$$4.3\ 10^{-4} R < r < R \tag{6}$$

which covers the essential part of the plastic zone. The region $r<4.3\ 10^{-4} R$ where the approximation cannot describe the displacements is generally insignificant when compared of the extension of the process region.

One may write the solution for modus I and a perfectly plastic

material [5] on the form:

$$\frac{v_a E}{r\sigma_Y} = \text{const.} \quad \ln \frac{eR}{R} \tag{7}$$

and then by using simple curve fitting one obtains

$$v_a = 3.11 \frac{\sigma_Y}{E} r \ln \frac{eR}{r} \tag{8}$$

and

$$R = 0.122 \, (K_I/\sigma_Y)^2 \tag{9}$$

Figure 3 shows that the approximation is good within the region

$$0.005 \, (K_I/\sigma_Y)^2 < r < 0.13 \, (K_I/\sigma_Y)^2 \tag{10}$$

The node closest to the crack tip is excluded. The difficulties in obtaining a consistant result here can be explained by the relative coarseness of the mesh at this point. The amplitude 3.11 can be compared with the value 2.76 for the perfectly plastic material which was determined for the case of small scale yielding through an examination of the velocities in the Prandtl slip line field [5].

It should be emphasized that the disturbing field generated by the process region itself cannot be considered due to the assumption that this region is a singular point. Thus it is in fact assumed both that the logarithmic field embeds the process region and that the region in which the stress and strain field is significantly affected by the presence of a true, non point shaped, process region is sufficiently small.

The steady state solution as regards stresses and strains is depending neither on the crack growth rate nor on any higher time derivatives of the crack length. Therefore a characteristic of the steady state

solution is that there is a direct proportionality between the crack growth rate and the stress and strain rates. The solution is valid for small crack growth rates including the arrested crack. Due to the self similarity of the asymptotic solution one may describe the situation in the crack tip neighbourhood by the parameter R or equivalently by the displacement, the stress, etc. at a certain distance from the crack tip. Similarly the strain rate at a certain distance from the crack tip might be chosen for a one parameter describing the near tip situation (cf. [6]) but this specific choice does not provide any further information what so ever as compared with any other among the variety of equivalent choices.

The analysis reported here start at the steady state situation that was obtained by means of a moving mesh technique. The obtained stress and strain field was used at the beginning of a FEM analysis at which the remote load (1) was removed in several small steps.

Unloading - reloading with overlapping crack surfaces

In a first attempt restrictions were not imposed as regards crack surface displacement. The result is in error in that it implies overlapping of the crack surfaces (see Fig. 4) but this is not unexpected as was indicated by a linear estimation in [2]. The result shows that the region of overlapping crack surfaces increases rapidly starting at remote load about 0.2 of full load K_{Io}. It is also obvious at inspection of the large displacement gradients near the crack tip that strains are localized in a process similar to crack tip blunting, but here as the load is decreased. One also note that the displacements are almost constant over the crack surface in the crack tip neighbourhood when the remote load is completely removed. Initially during unloading the complete plate is elastic. It is not until the external load drops below about 0.7 of the full load that the first

plastic integration point is obtained (see Fig. 5).

Figure 5 also shows the crack surface during reloading. For comparison dotted lines show the displacement at corresponding external load during unloading. As a curiosity one observes that (although significant differences arise during reloading-unloading) when full load is restored the result is very similar to the steady state result at least as regards the crack surface displacements. The plastic zone at full load shown in Fig. 6 is also observed to be rather similar to the plastic zone at steady state.

This solution is of fear for a significant influence of the extensive overlapping, only used as a reference for further work.

Unloading - reloading with crack surfaces in contact

The result during unloading when contact forces is introduced to prohibit overlapping is displayed in Fig. 7. The deviations in displacement due to crack surface contact are, when compared with Fig. 4, observed to be small outside the contact region. It is also observed that the extension of the contact region is rather small for loads larger then about $0.4K_{Io}$. At the end of the analysis when the remote load is completely removed crack surfaces are in contact along the crack as far as is covered by the element mesh.

Immediately as the load is decreased from the steady state situation the complete plate becomes elastic and it is not until below $0.4K_{Io}$ that the material behaviour becomes plastic at the first integration point. Fig. 8 shows the plastic zones at $0.6K_{Io}$, $0.4K_{Io}$, $0.2K_{Io}$ and when the

remote load is completely removed. The secondary plastic zone present at steady state remains elastic throughout the unloading process.

At the following analysis the initial load is restored. During this part, as in the first phase of the analyses, the crack is assumed not to grow. The reloading induced large changes in plastic strain distribution. The load had to be applied in 75 increments in order to keep the changes in strains at a reasonably low level during each increment.

Evidently the process is not reversible. A study of Fig. 10 reveals large deviations in the crack surface displacement during reloading compared with unloading at corresponding loads. Excessive blunting of the crack tip is observed. This is manifested by a displacement of the node closest to the crack tip $v=0.30K_I^2/E\sigma_Y$ which can be compared with the result for a static virgin crack $v=0.33K_I^2/E\sigma_Y$ (cf. [7]). At a larger distance from the crack tip the deviation from the steady state result decrease very slowly, e.g. from $\Delta v=0.08K_I^2/E\sigma_Y$ at $r=0.04(K_I/\sigma_Y)^2$ to $\Delta v=0.06K_I^2/E\sigma_Y$ at $r=0.13(K_I/\sigma_Y)^2$. When studying the extension of the plastic zones one is struck by the early appearance of the secondary plastic zone (see Fig. 10). This zone that is absent during the entire unloading phase now increases continuously during the reloading to assume about the same height at full load as previously at the steady state. The primary plastic zone, surrounding the crack tip, appear first at 0.6 of full load and increases rapidly during the remaining part of the reloading part to finally assume about the same extension about as that found at steady state.

Continued crack growth at unchanged load. $K_I = K_{Io}$

Continued crack growth is studied by means of a nodal relaxation technique. In order to eliminate errors due to the change of FEM technique, node relaxation is first used to simulate crack growth

immediately following the moving mesh analysis [2], hence leaving out the removal and restorage of remote load.

The displacement is slightly larger here when the node relaxation technique is used then at the moving mesh technique (see Fig. 11). By plotting vE/σ_Y versus $\ln(eK_{Io}^2/r\sigma_Y^2)$ (cf. Fig. 12) one discovers that result is essentially identical if the node closest to the crack tip is excluded. The solution (8) and (9) represented by a straight line is included in the figure. The best approximation in the least square sence is given by:

$$v_a = 2.85 \frac{\sigma_Y}{E} r \ln \frac{eR}{r} \tag{11}$$

with

$$R = 0.166 (K_I/\sigma_Y)^2 \tag{12}$$

This solution is hereafter replacing the r^s depending solution for the displacements. The shape of the plastic zone remains almost constant (see Fig. 13). Only a slight deviation appear at the end of the analysis. In all 10 nodes were relaxed covering a distance $0.075(K_{Io}/\sigma_Y)$.

Continued crack growth at $K_I=0.6K_{Io}$.

A crack that experience steady state crack growth, then the load instantaneously decreased to $0.6K_{Io}$ followed by continued crack growth by relaxation of nodes is studied. Fig. 14 shows the displacements during the continued crack growth. The result before crack growth is included for comparison. As the first two nodes are relaxed the displacement for these decrease, i.e. the crack surfaces overlap. This is of course an unrealistic situation. The implications are not fully

understood and we are submitted to speculations. It might for instance be that a micro crack occurs first is formed ahead of the crack tip that later coalesce with the main crack or the main crack might even circumfere the region ahead of the crack tip.

Assuming that (11) defines the near tip field at crack growth also shortly after a load transient, the parameter R is easily obtained in Fig. 15. Through (12) the equivalent stress intensity factor performing the identical displacement field is obtained as well. The equivalent stress intensity factors are observed to change significantly, increasing from a very small value to a value very close to the value expected at steady state crack growth.

First plasticity occurs only at the former secondary plastic zone adjacent to the crack surface. Plasticity occurs in the crack tip neighbourhood when the next two nodes are relaxed and it is also at this moment that the displacements begins to increase. Fig. 16 shows the result for 2, 4, 6, 8 and 10 relaxed nodes. Finally when 10 nodes are relaxed the height of the plastic zone is $0.046(K_{Io}/\sigma_Y)^2$ which equals $0.13(K_I/\sigma_Y)^2$. This can be compared with the height $0.14(K_{Io}/\sigma_Y)^2$ at steady state.

Continued crack growth at $K_I = 0.6K_{Io}$ after an intermediate unloading-reloading process

Figure 17 shows the displacements for 0, 2, 4, 6, 8 and 10 nodes relaxed. Compared with the result without unloading-reloading the displacements are now larger and the crack surfaces did not overlap at any stage of the continued crack growth. In a $vE/r\sigma_Y$ versus $\ln(eK_{Io}^2/r\sigma_Y^2)$ diagram (Fig. 18) R is found and the equivalent stress intensity factor is obtained. The crack surface displacements correspond to a small scale yielding case $K_I = 0.38K_{Io}$ as the two first nodes are relaxed and

finally $K_I = 0.73K_{Io}$ as 10 nodes are relaxed. Thus K_I is about 20% larger than expected ($K_{Io} = 0.6K_{Io}$). This cannot yet be explained. It cannot be explained by the increase in K_I due to the increased crack length considering the finite geometry covered by the element mesh. This would only account for on increase of about 1.2%. A further analysis is needed to reveal if the result for crack growth before and after an intermediate unloading-reloading converges as the amount of crack growth increases.

The plastic zones is surrounding an elastic region in the crack tip vicinity after relaxation of the first two nodes (see Fig. 19). During the relaxation of the next 8 nodes the elastic region, at the site of the crack tip during the unloading-reloading process, remains elastic. When 10 nodes are relaxed the shape of the primary plastic zone is rather similar to the plastic zone in Fig. 16, i.e. without intermediate unloading-reloading.

Continued crack growth at $K_I = K_{Io}$ after an intermediate unloading-reloading process

It is interesting to compare the last case with the reference case for which the moving mesh technique was instantaneously replaced with the node relaxation technique for steady state solutions since unloading-reloading has been recommended [1] as a method for breaking conductive bridges at the crack surface. It is assumed that these are resposible for an appearant, but not true decrease in crack length as measured by the potential drop method. As an accompanying effect the crack appears to be slightly larger after the unloading-reloading cycle (see Fig. 20).

The excessive blunting observed at the reloading process results after some amount of crack growth in an indentation of the width 0.018

$(K_I/\sigma_Y)^2$ and the depth about $0.32K_I^2/E\sigma_Y$ at 4 relaxed nodes and the width $0.022(K_I/\sigma_Y)^2$ and the depth about $0.29K_I^2/E\sigma_Y$ at 10 relaxed nodes (see Fig. 21). The crack surface displacements are larger than at steady state on the trailing side of the indentation and the difference is almost constant for $x>-0.15(K_I/\sigma_Y)^2$. Thus the difference is $0.09K_I^2/E\sigma_Y$ at $x=-0.04(K_I/\sigma_Y)^2$ and $0.07K_I^2/E\sigma_Y$ at $x=-0.10(K_I/\sigma_Y)^2$ before continued crack growth and $0.10K_I^2/E\sigma_Y$ at $x=-0.04K(K_I/\sigma_Y)^2$ and $0.08K_I^2/E\sigma_Y$ at $x=-0.10(K_I/\sigma_Y)^2$ after 10 relaxed nodes.

In a $vE/r\sigma_Y$ versus $\ln(eK_I^2/r\sigma_Y^2)$ diagram (Fig.22) the resulting displacements at the advancing side of the indentation are fairly collected and seems to be very little different from the result at steady state.

The plastic zone (see Fig. 23) is, as was observed at continued crack growth for the lower load $0.6K_{Io}$, avoiding the region in the immediate surrounding of the position of the crack tip at the unloading-reloading process, i.e. $x = 0$. Finally as 10 nodes are relaxed the shape of the plastic zone resembles the one found at steady state.

Result and discussion

It has been possible to apply the approximation (8) for the displacements of the new crack surface created at crack growth after a few different transient loads. The approximation coincides well with the obtained FEM results accept may be for the result as the first two nodes are relaxed and generally when the node nearest the crack tip is excluded. The near tip field described by (8) is related to the near tip field at steady state through the estimation of R which for small scale yielding steady state equals $0.16(K_I/\sigma_Y)^2$. These values for the equivalent small scale yielding K_I is plotted versus crack length and compared with the stress intensity factor for the surrounding elastic

field, in Fig. 24 a - d.

Estimation of the crack growth after a sudden change of the remote load can be made through the knowledge of the crack growth at small scale yielding. The computed crack length should however be handled with caution for cases where the displacements are very small or even negative at the initiation of continued crack growth (e.g. where r>R). Thus it is emphasized that the initiation after a decrease in remote load (e.g. to $0.6K_{Io}$) could not be explained while the result actually implied that the crack should remain arrested. This is in contradiction with experimental results showing continued crack growth after some delay. If the delay at initiation is excluded or estimated by other means, it is believed that the following crack growth can be estimated by an examination of the near tip displacement field. The amount of crack growth that should be excluded does of course depend on the character of the transient load. For the situation in Fig. 24 b) could be of a size say $0.008K(K_I/\sigma_Y)^2$. For a $K_I=\sqrt{a}/2.5\ \sigma_Y$ i.e. at the ASTM limit for linear fracture mechanics this is 0.5% of the crack length for an edge crack. It is here reminded that if the grain size or what might be considered as the size of the process region is large than $0.008(K_I/\sigma_Y)^2$ that amount of crack growth should be excluded instead because of the weak foundation for the analysis at the length scale of the process region.

Acknowledgement

The work was sponsored by the Swedish Nuclear Power Inspectorate. The authors wish to express their gratitude for this support.

REFERENCES

---

[1] L. Ljungberg, Private communication, 1987.

[2] P. Ståhle and F. Nilsson, "A comparative study of two steady-state situations at a quasi-statically growing crack in a stainless steel", report from Dept. of Solid mech. UTH, 1987.

[3] P. Ponte Castañeda, J. Mech. Phys. Solids 35, 1987.

[4] J. Huchinson and J. Amazigo, J. Mech. Phys. Solids 25, 1977.

[5] W. Drugan, J. Rice and T-L. Sham, J. Mech. Phys. Solids 30, 1982.

[6] W. Cullen, G. Gabetta and H. Hanninen, "A Review of the Models and Mechanisms for Environmentally-Assisted Crack Growth of Pressure Vessel and Piping steels in PWR Environments", report: NUREG/CR 4422, MEA-2078, RE, R5, U.S. Nuclear Regulatory Commission, Washington, D.C. 20555, 1987.

[7] J. Rice and E. Sorensen, J. Mech. Phys. Solids 26, 1978.

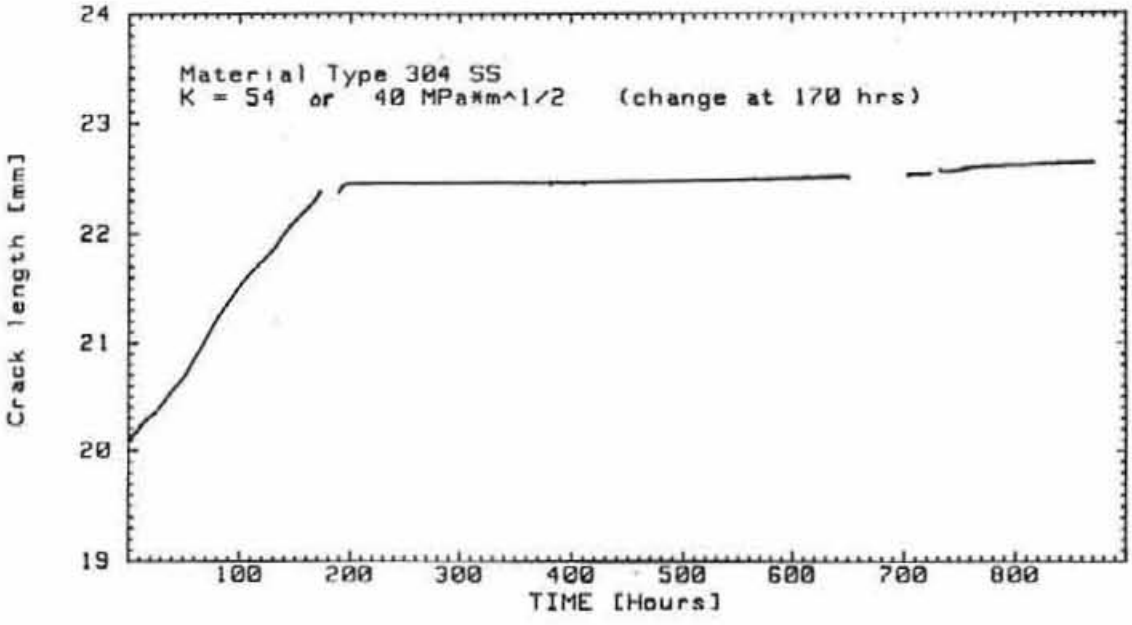

Fig. 1 Crack length (measured by a potential drop method) versus time. At a sudden drop in load at A the crack is arrested until after a few hundred hours (at B) when the crack starts growing very slowly.

Fig. 2 Components of stress σ_y, σ_θ and $\tau_{r\theta}$ found at the FEM analysis [2], for the asymptotic solution [3] and for the perfectly plastic material [5].

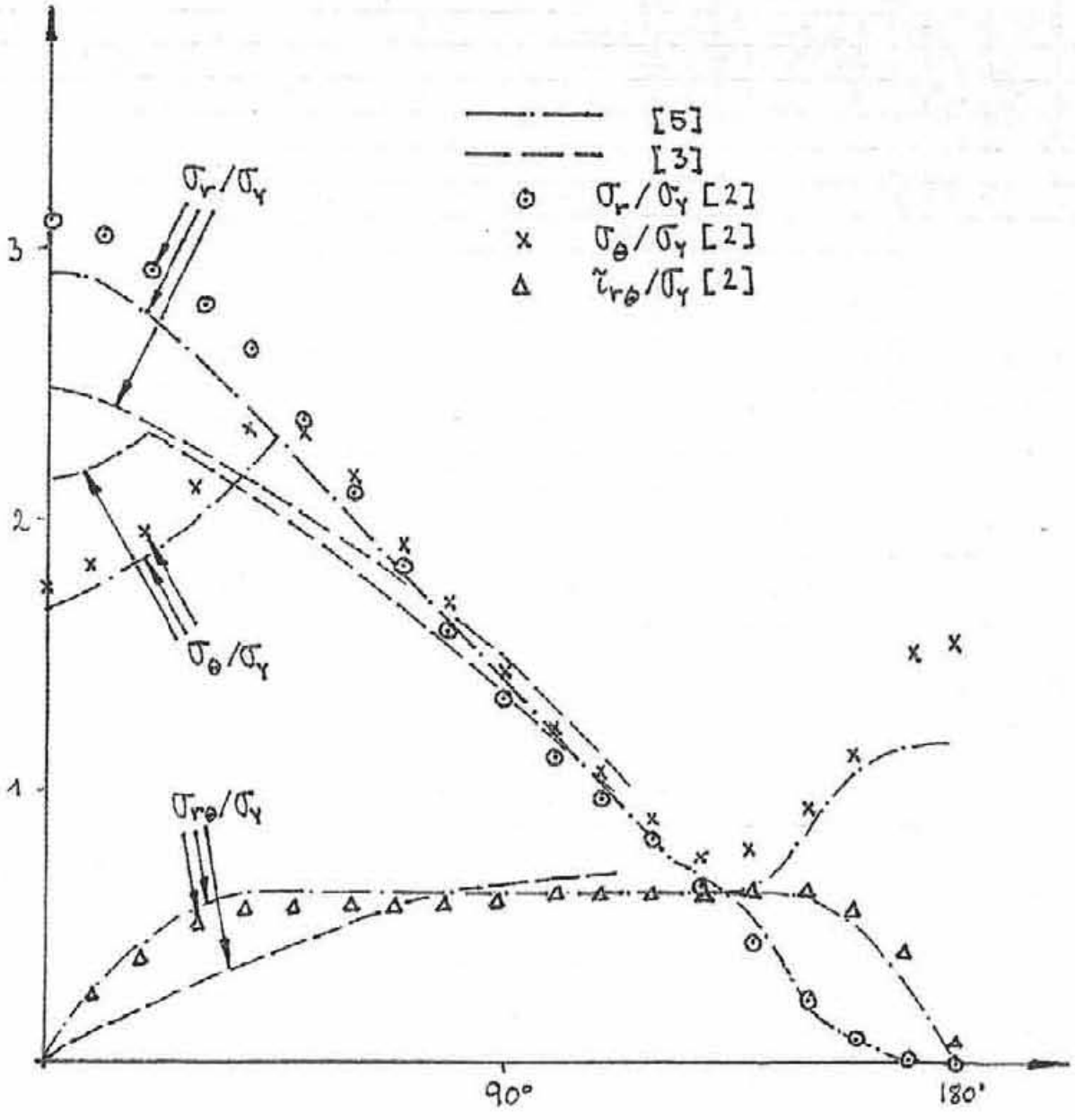

Fig. 3 Ratio v/r versus $\ln(eK_{Io}^2/r\sigma_Y^2)$ at steady state. The approximation (8) is represented by a straight line. The result [5] for the perfectly plastic material is included for comparison. The result $v \sim r^{0.9203}$ [3] is ambiguous as regards amplitude. Here the two choices $v = 0.4K_{Io}^{2-2s}\sigma_Y^{2s-1}r^s/E$ and $0.09K_{Io}^{2-2s}\sigma_Y^{2s-1}r^s/E$ where $s = 0.9203$ are shown.

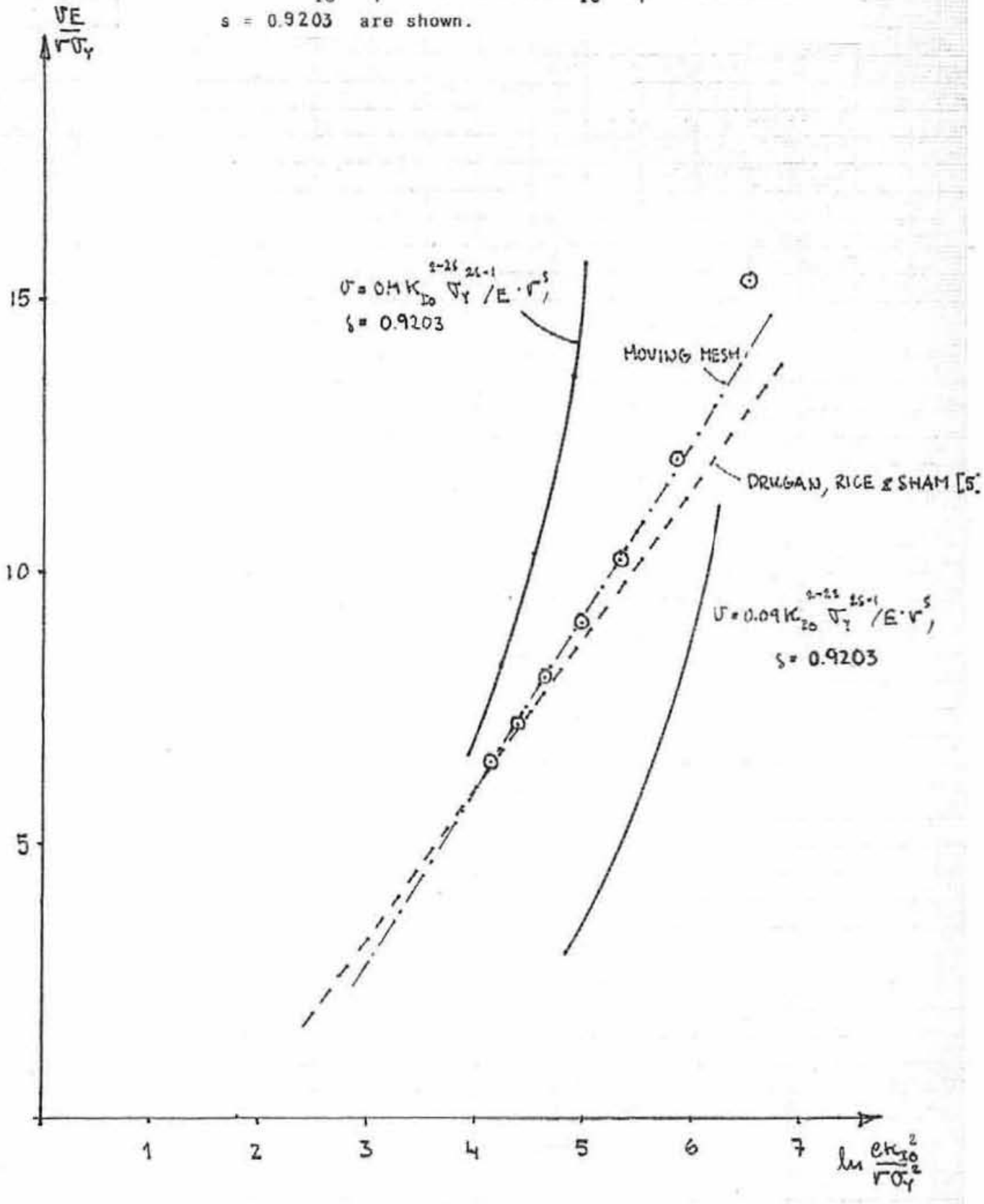

Fig. 4 Displacements at steady state and during unloading and reloading. Overlapping of the crack surfaces is not prohibited. When the load is completely removed ($K_I = 0$) the overlapping zone covers the entire crack. Excessive blunting is observed during reloading. Overlapping of the upper and lower crack surfaces disappears at $K_I = 0.4K_{Io}$.

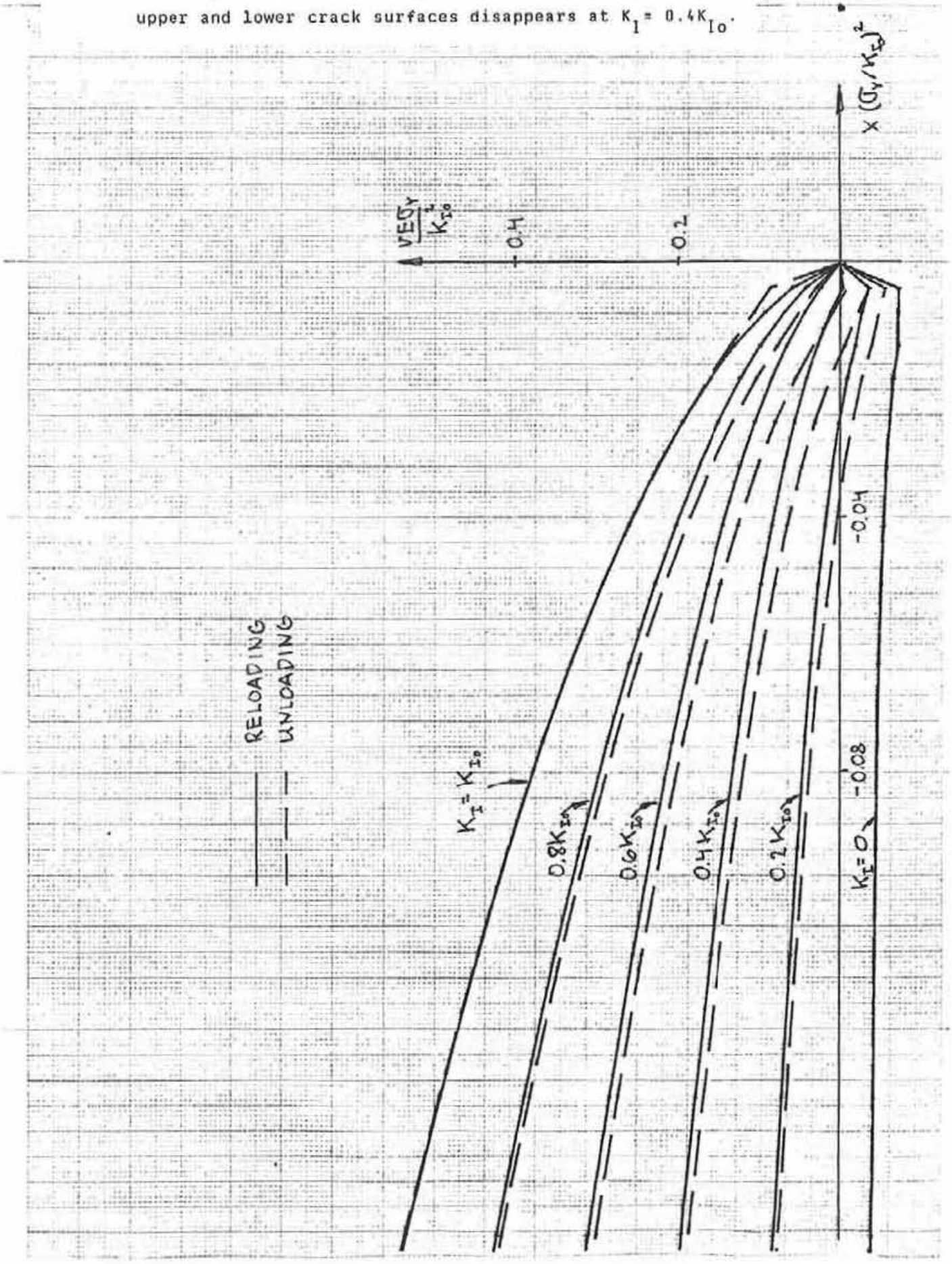

Fig. 5 Shape of the plastic zone during unloading. Overlapping is not prohibited.

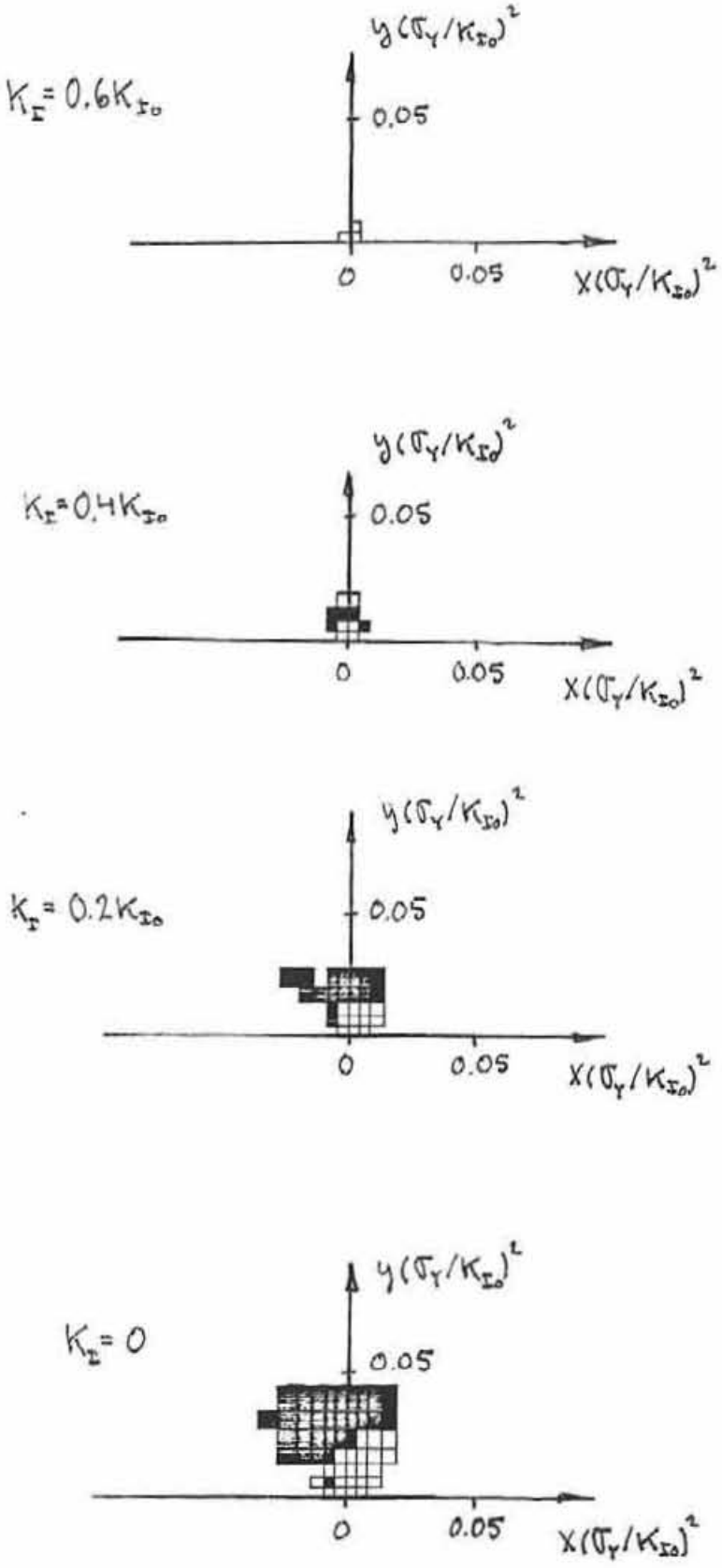

Fig. 6 Shape of the plastic zone during reloading. Overlapping is not prohibited.

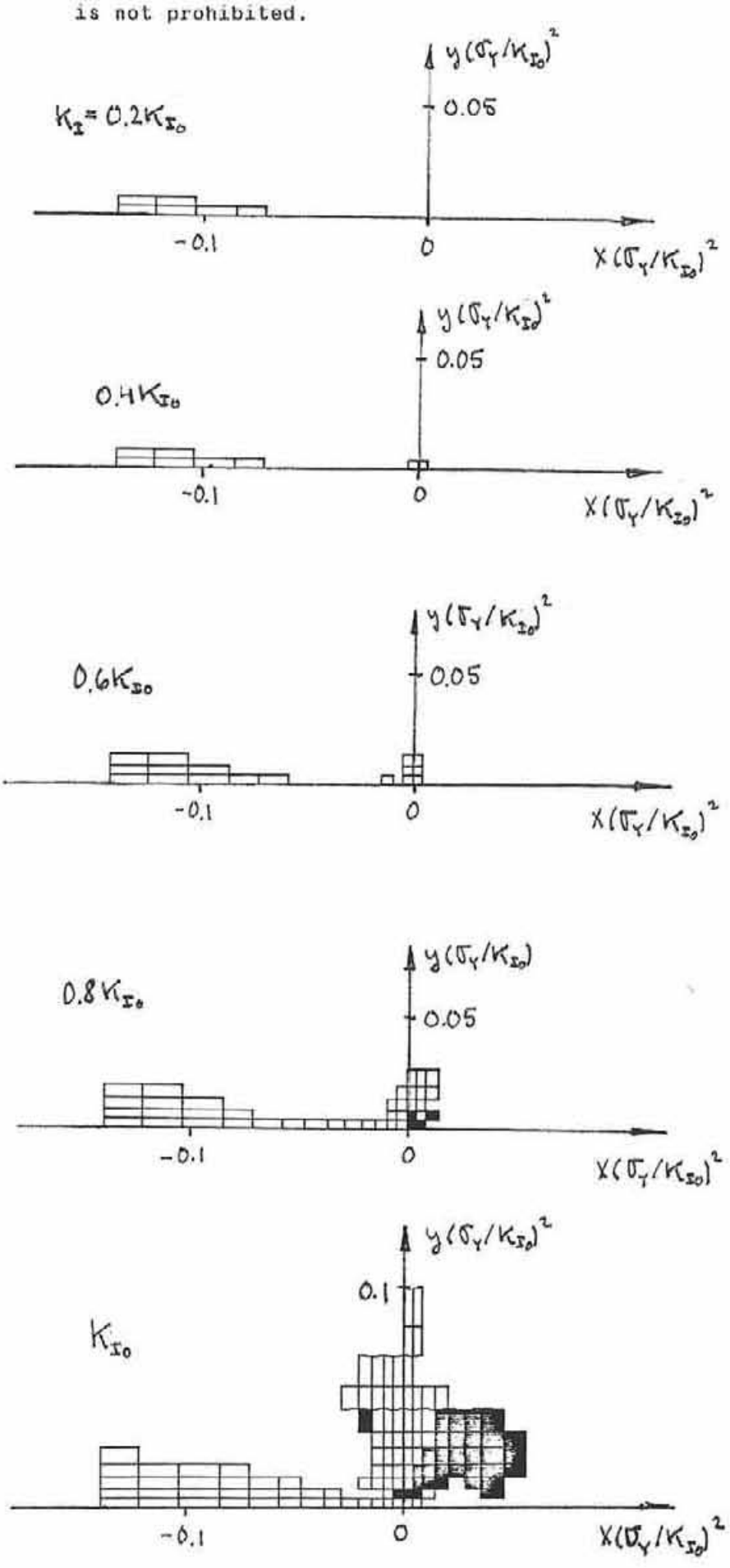

Fig. 7 Displacements during unloading. The first node is in contact with the lower crack surface at $K_I = 0.4K_{Io}$. The entire crack is closed at $K_I = 0$.

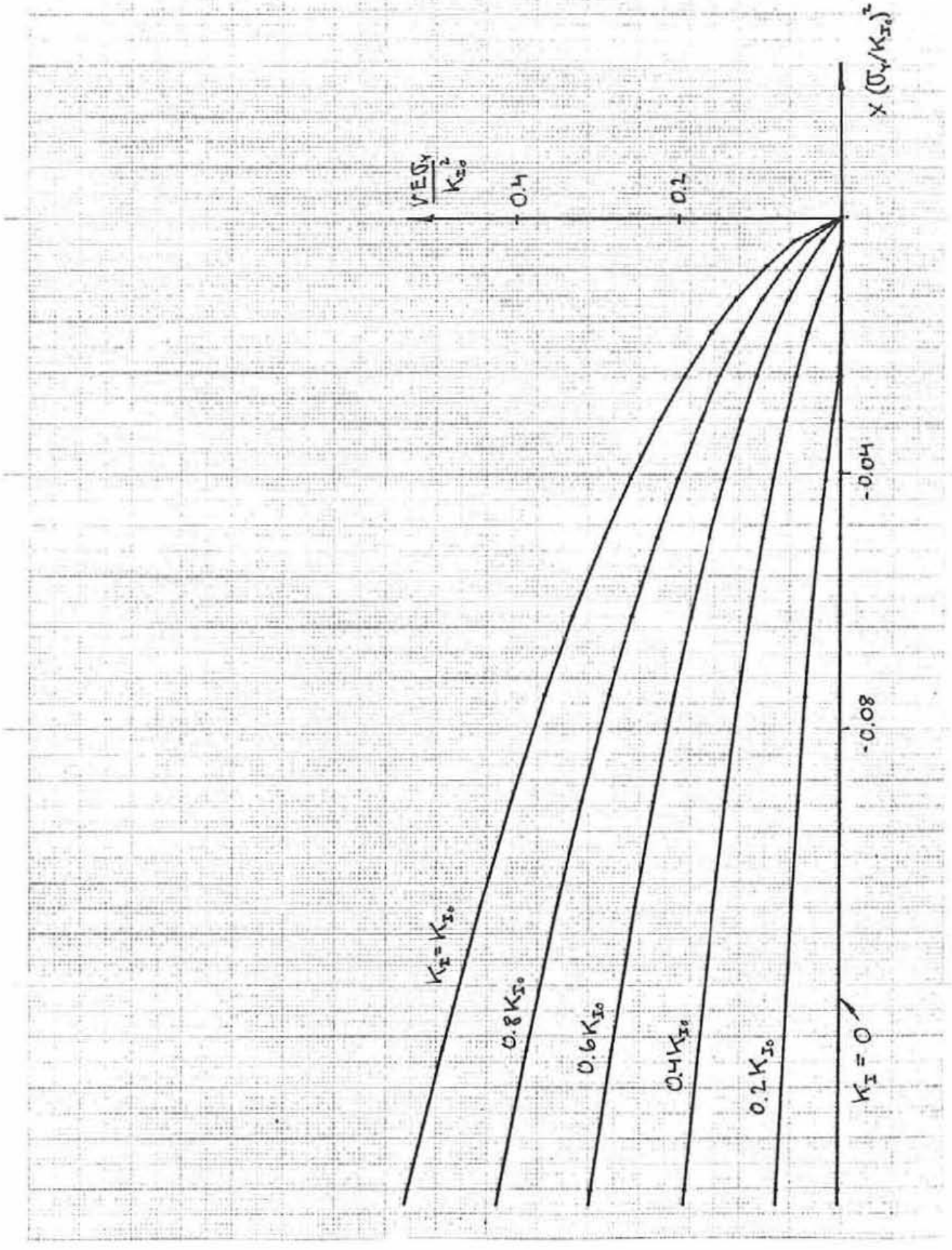

Fig. 8 Shape of the plastic zone during unloading. The entire plate remains elastic until $K_I = 0.2K_{Io}$.

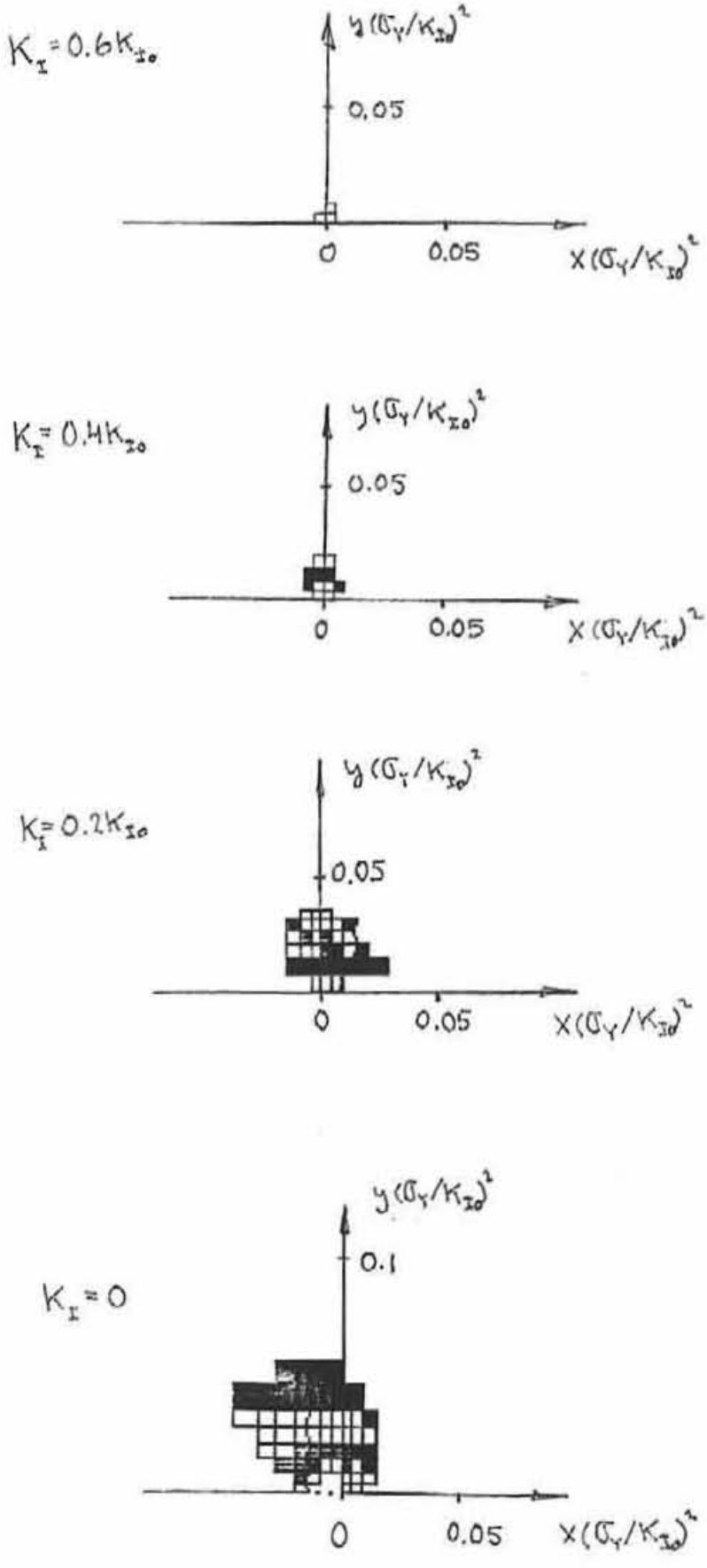

Fig. 9 Displacements during reloading. The contact between the upper and lower crack surfaces disappears immediately as the load is increased.

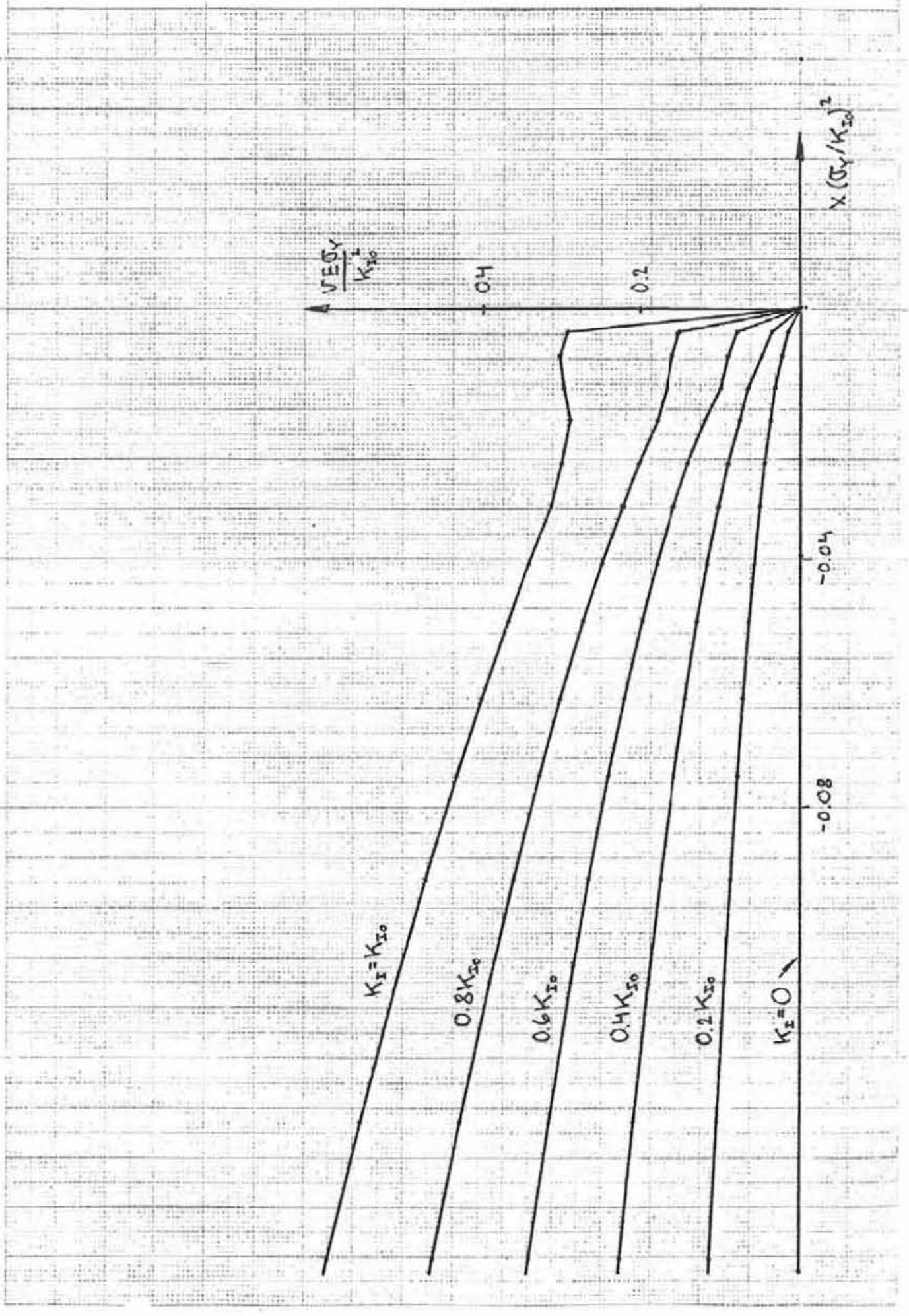

A4 – 1 X 1 mm

AGE 22

Fig. 10 Shape of the plastic zone during reloading. The first integration points that become plastic appear in the former secondary plastic zone.

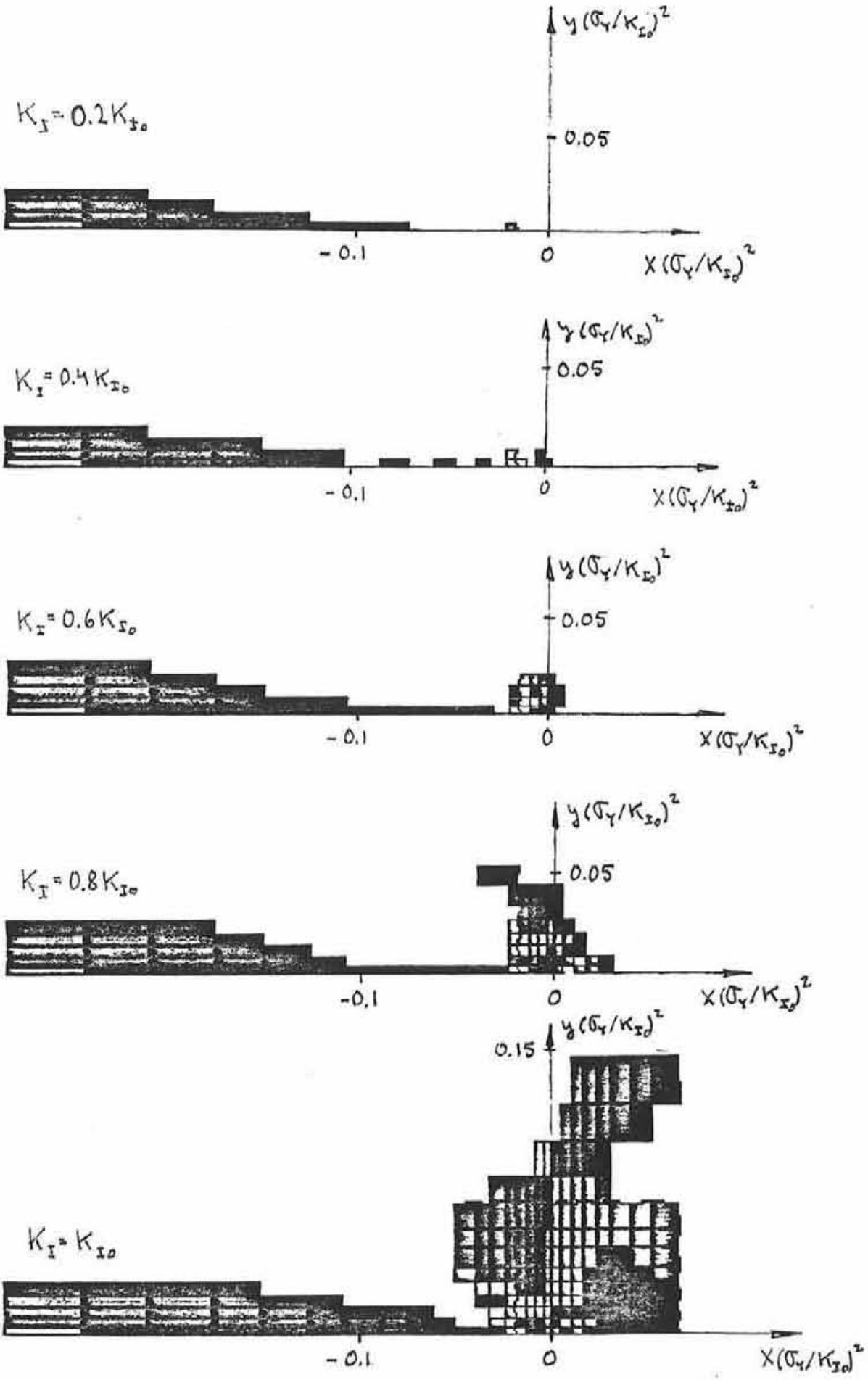

Fig. 11 Displacements during node relaxation immediately following the steady state solution obtained by the moving mesh technique.

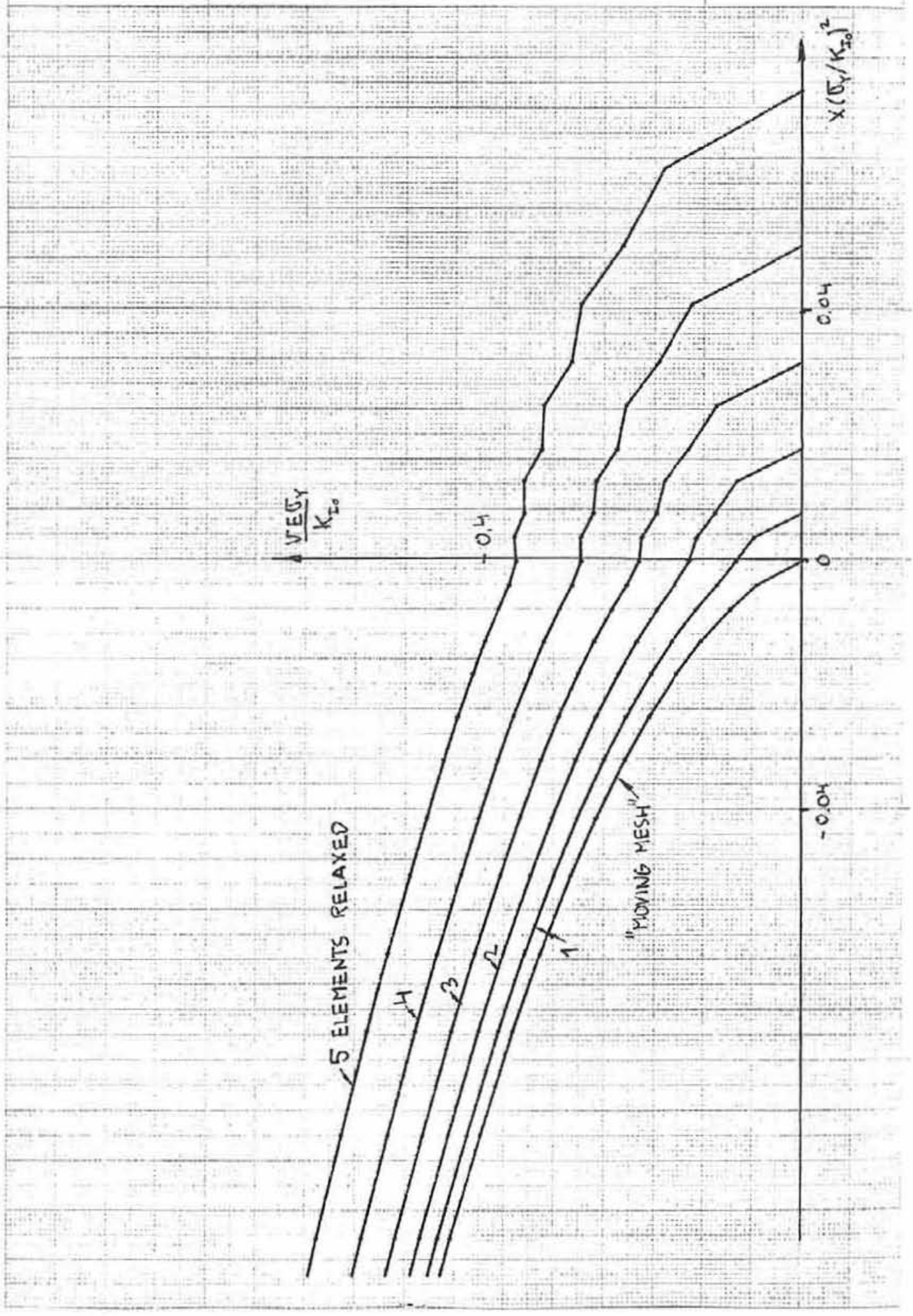

Fig. 12 vE/ro_Y versus $\ln(eK_{Io}^2/ro_Y^2)$ for the situations in Fig. 11.

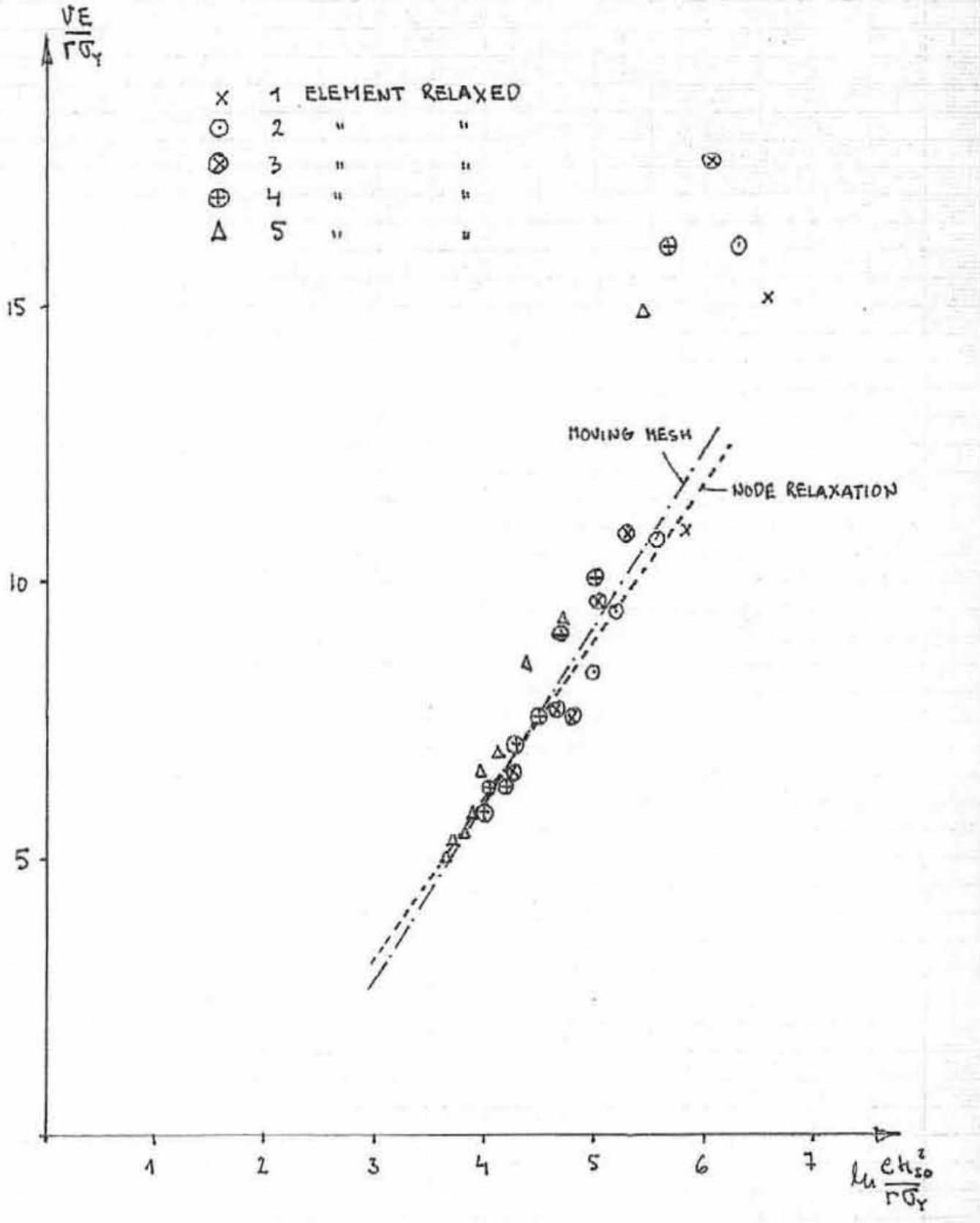

Fig. 13 Shape of the plastic zone for the situations in Fig. 11.

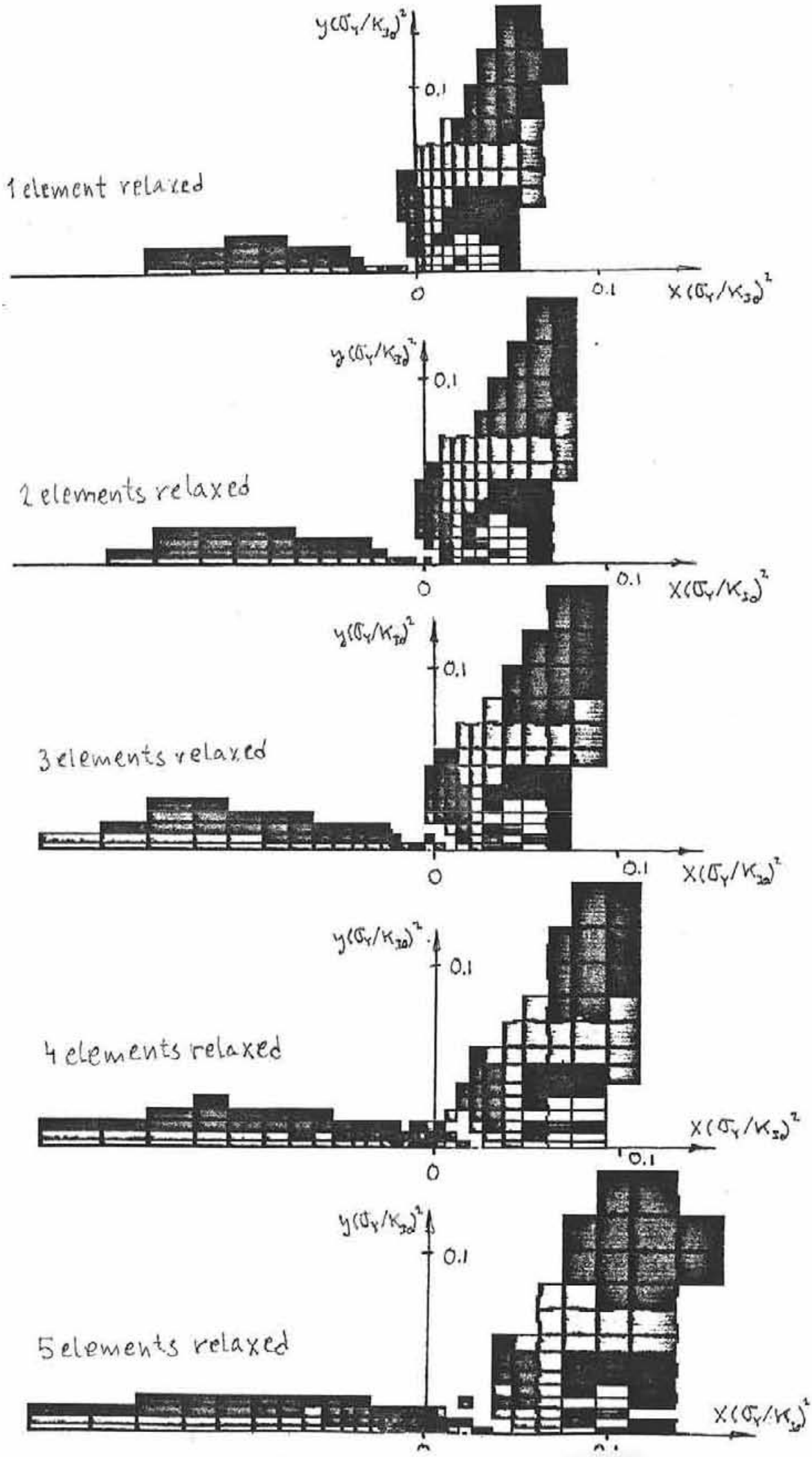

Fig. 14 Displacements during node relaxation after unloading to $K_I = 0.6K_{Io}$.

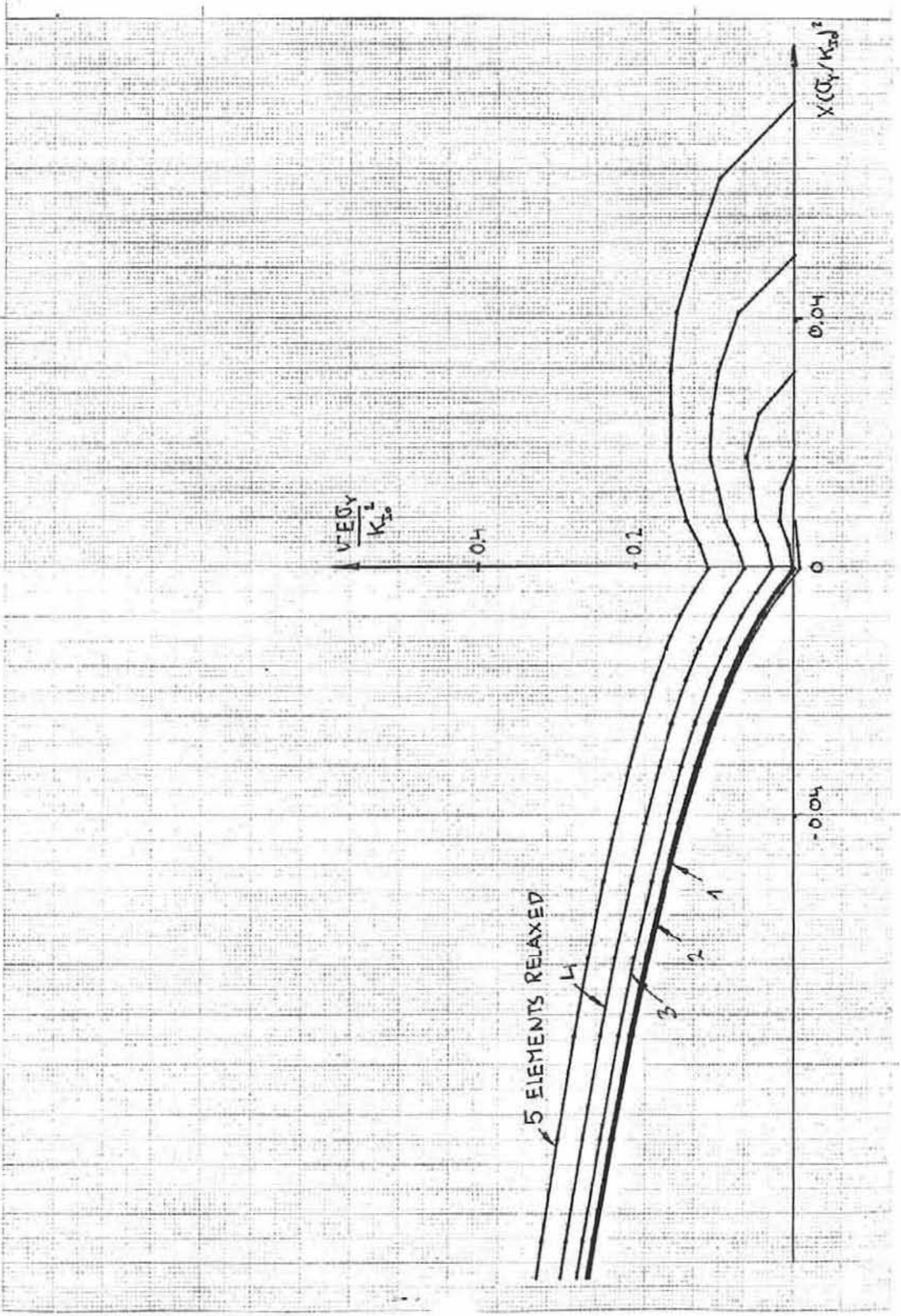

Fig. 15 $vE/r\sigma_Y$ versus $\ln(eK_{Io}^2/r\sigma_Y^2)$ for the situations in Fig. 14.

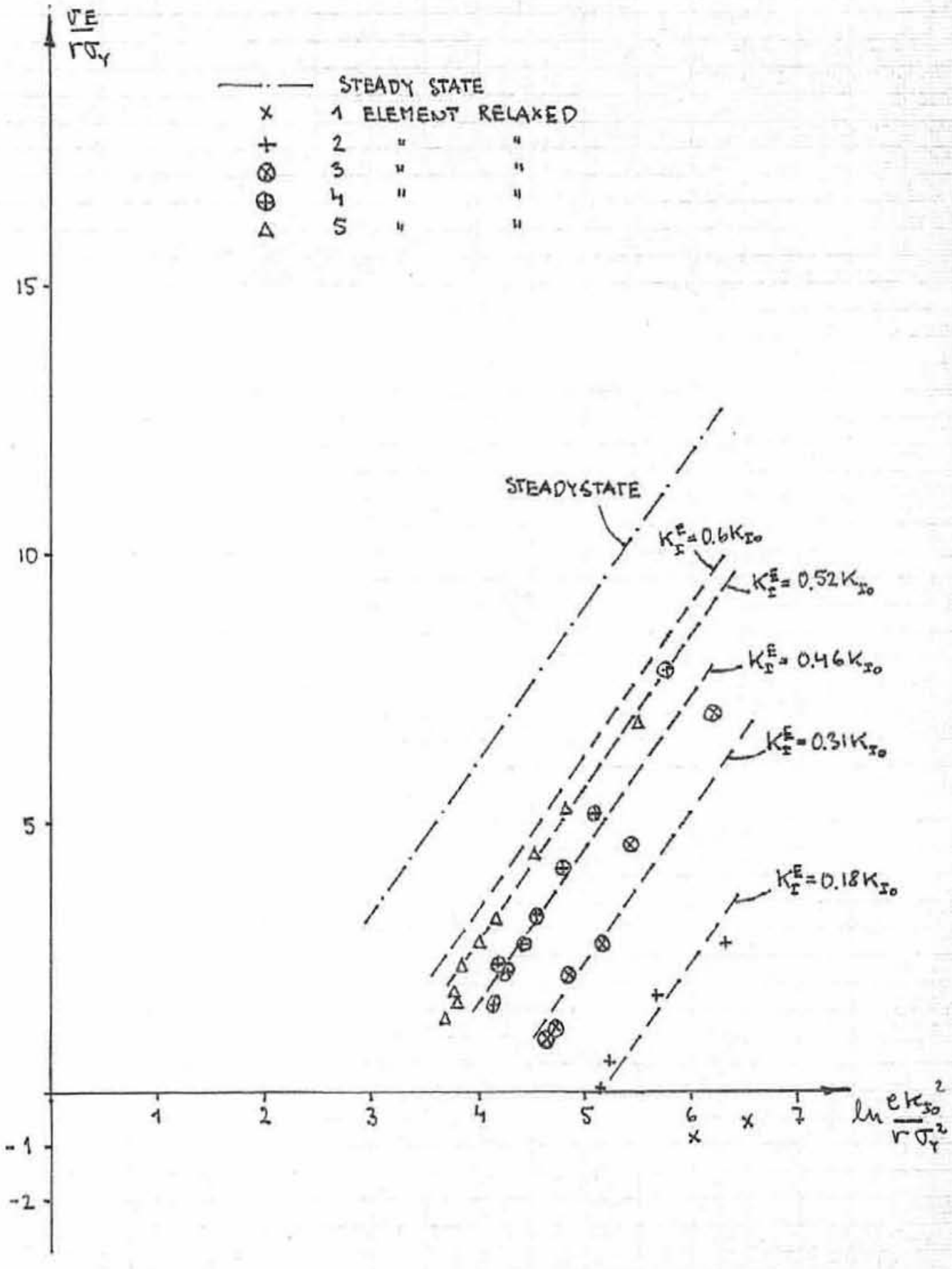

Fig. 16 Shape of the plastic zone for the situations in Fig. 14.

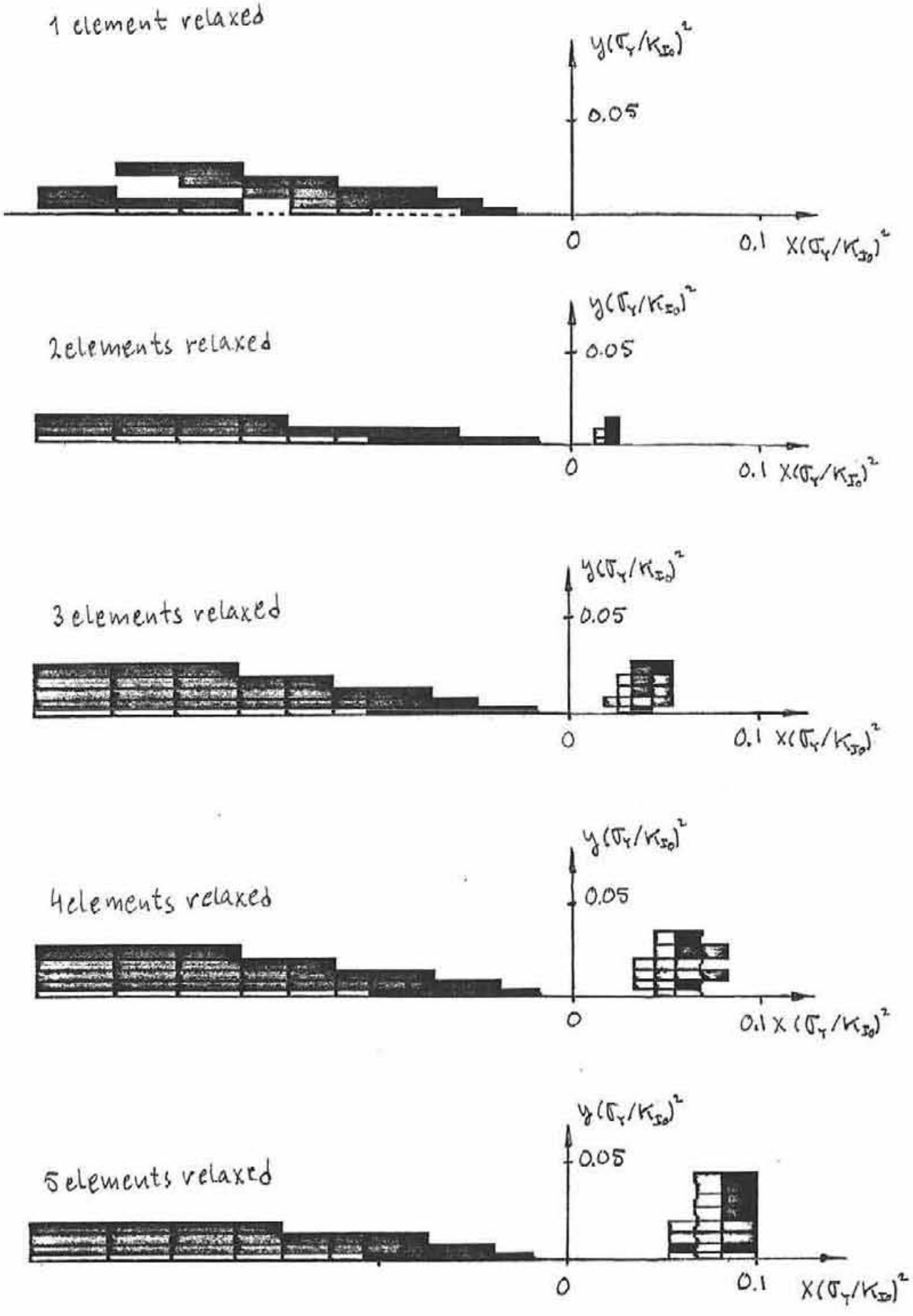

Fig. 17 Displacements during node relaxation after unloading to $K_I = 0$ and reloading to $K_I = 0.6K_{Io}$.

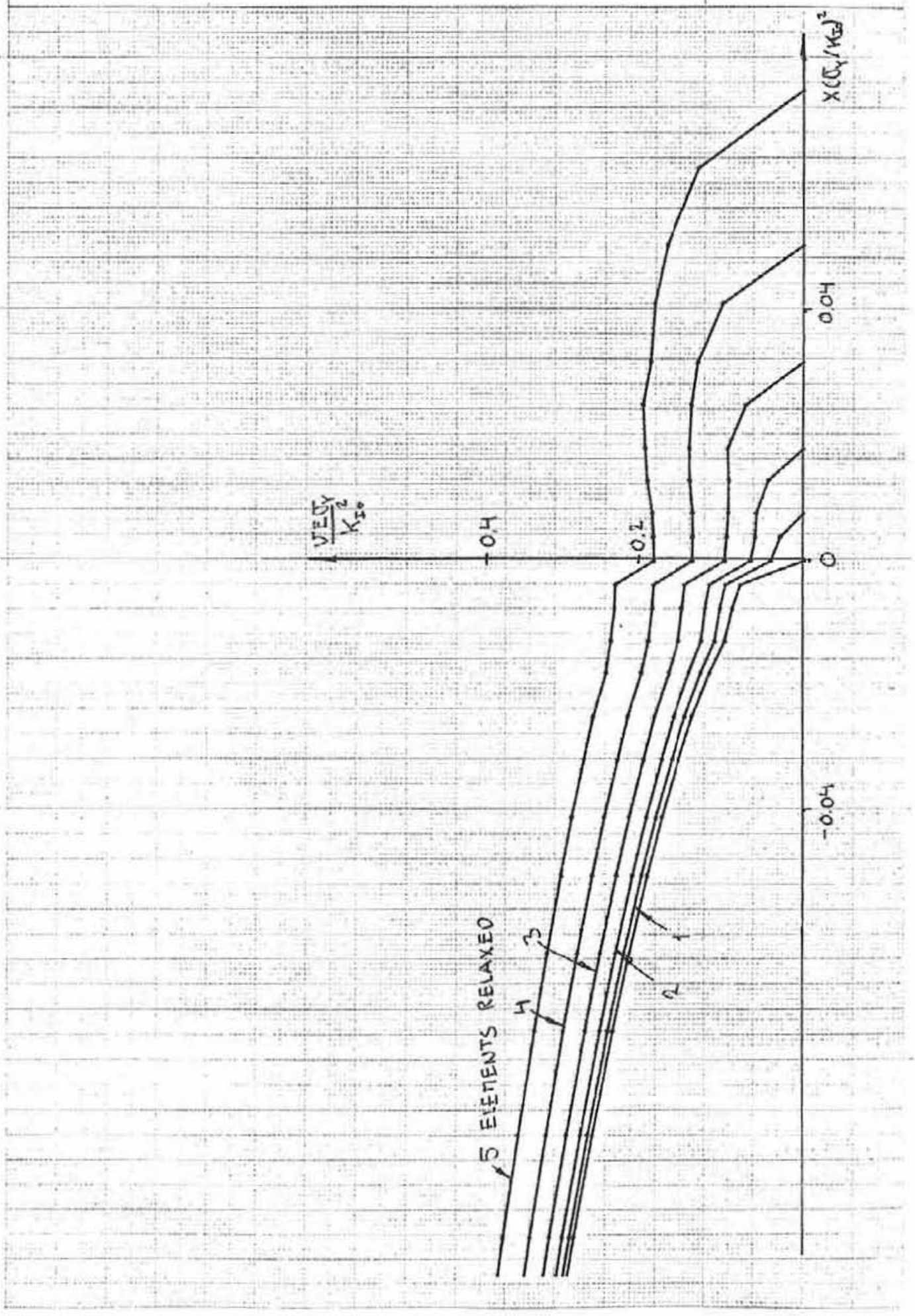

Fig. 18 $vE/r\sigma_Y$ versus $\ln(eK_{Io}^2/r\sigma_Y^2)$ for the situations in Fig. 17.

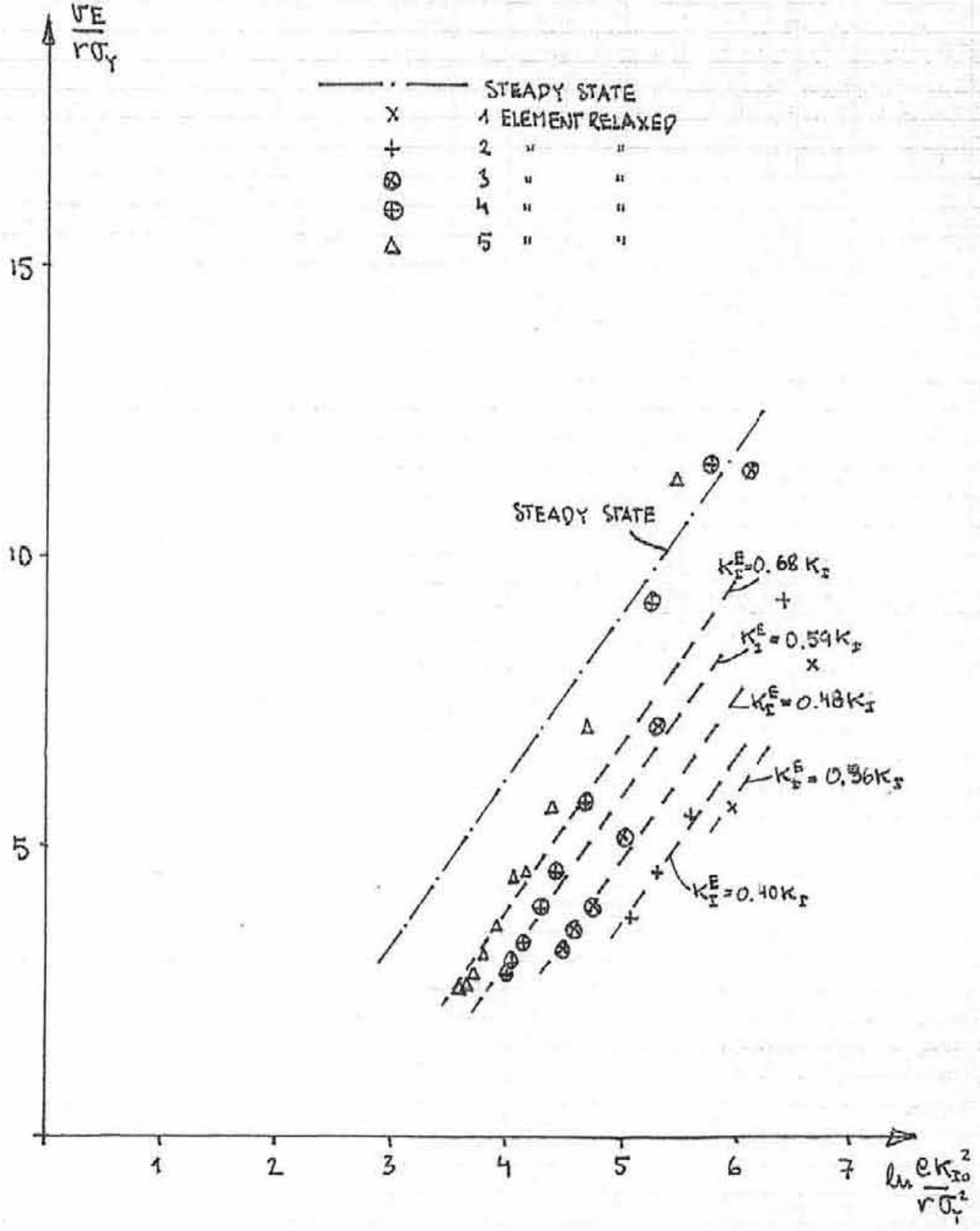

Fig. 19 Shape of the plastic zone for the situations in Fig. 17.

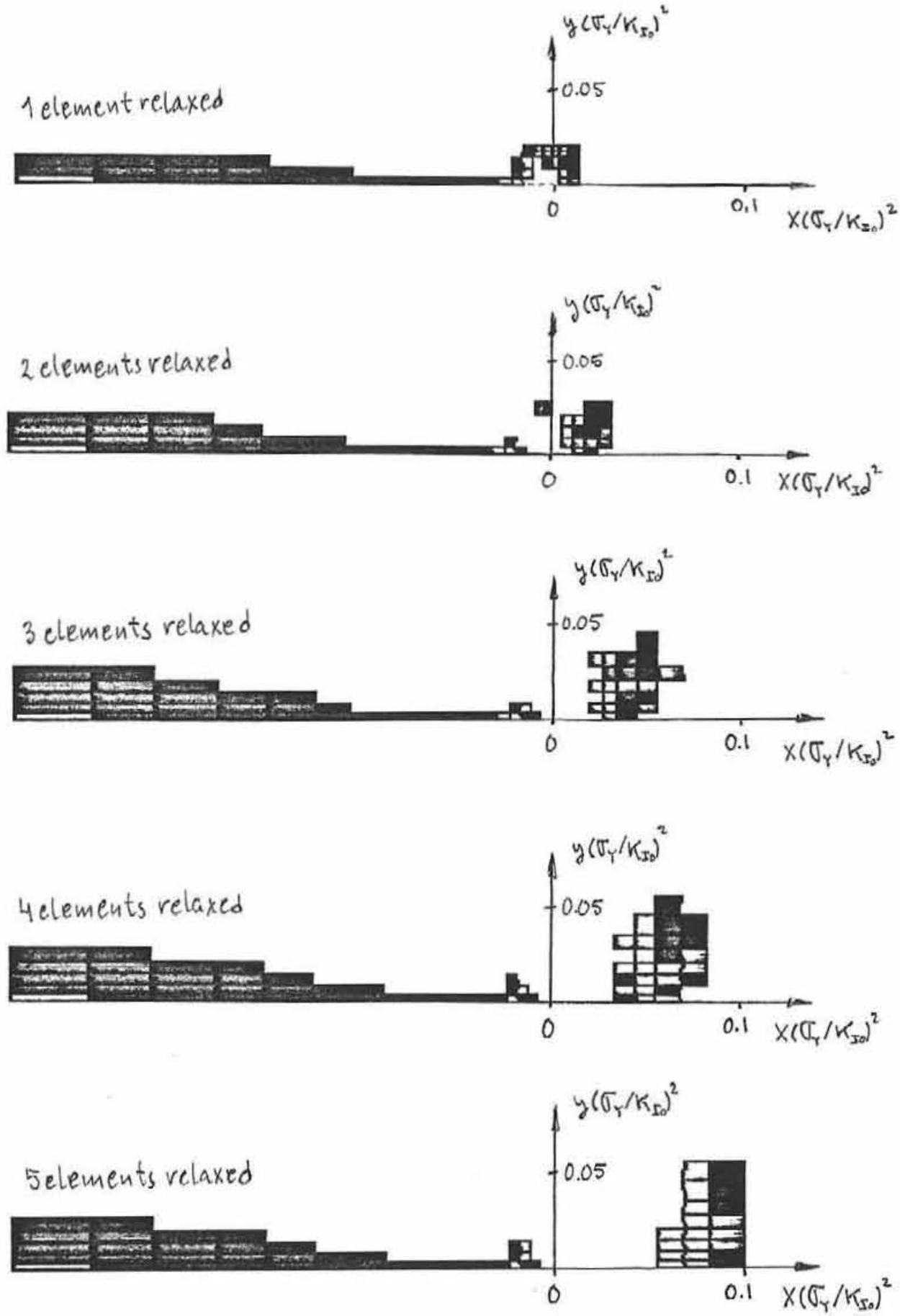

PDT Voltage over Crack in Constant Load Test XV (Environment I, 0.1 ppm H_2SO_4)

There was no crack growth during the first 125 hrs of the test

The data acquistion system failed during 2 periods of time

Bars in top of graph show periods of time when load was cycled to initiate cracking

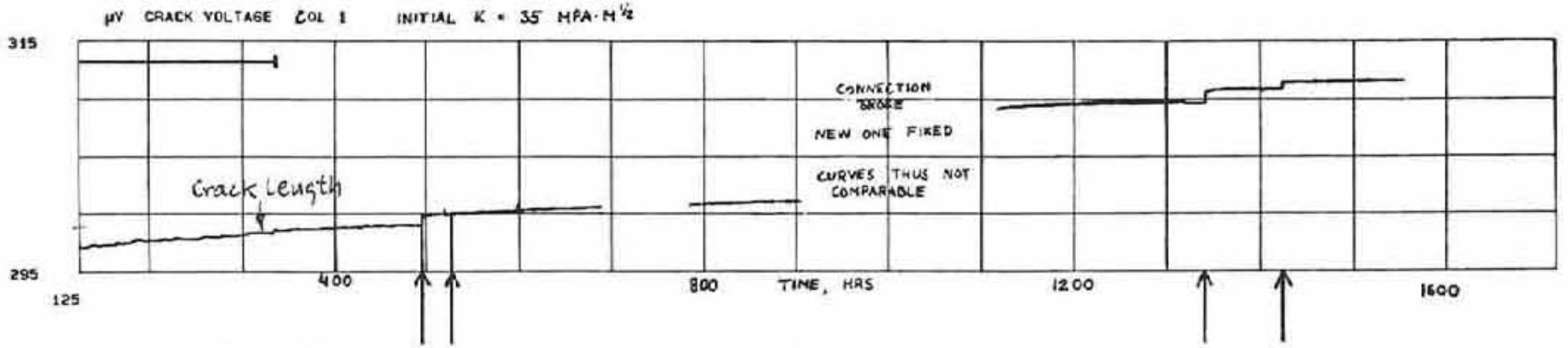

At points of time marked by arrow load was temporarily decreased to a value corresponding to K_I = 12 MPa·m½

Fig. 20 Crack propagation in a constant load specimen tested in normal BWR water with 25 ppb H_2SO_4 at 288°C. Initially the specimen was loaded to K_{Io} = 54 MPam$^{1/2}$. By 170 hours load was decreased to K_I = 40 MPam$^{1/2}$.

Fig. 21 Displacements during node relaxation after unloading to $K_I = 0$ and reloading to $K_I = K_{Io}$.

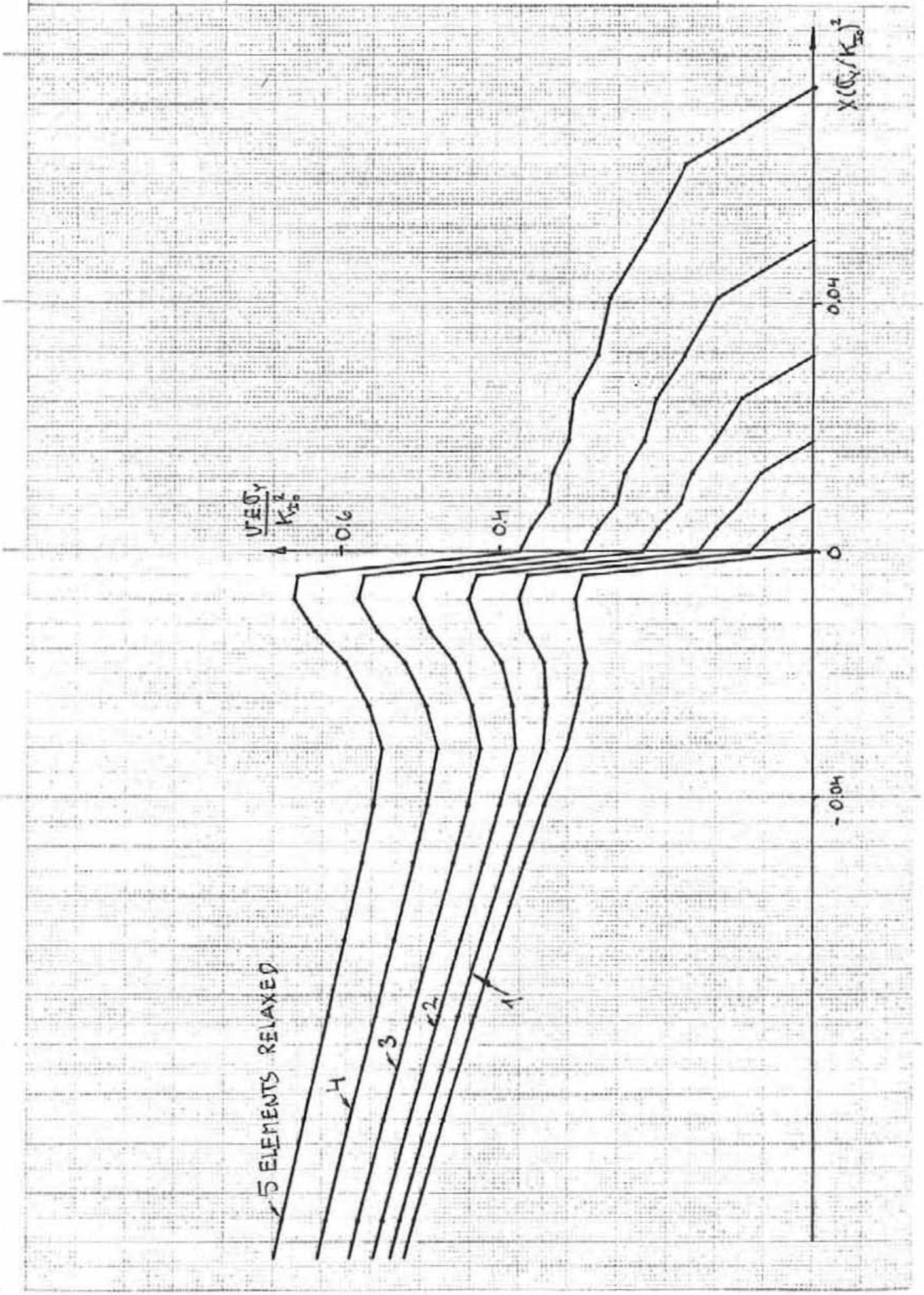

Fig. 22 $vE/r\sigma_Y$ versus $\ln(eK_{Io}^2/r\sigma_Y^2)$ for the situations in Fig. 21.

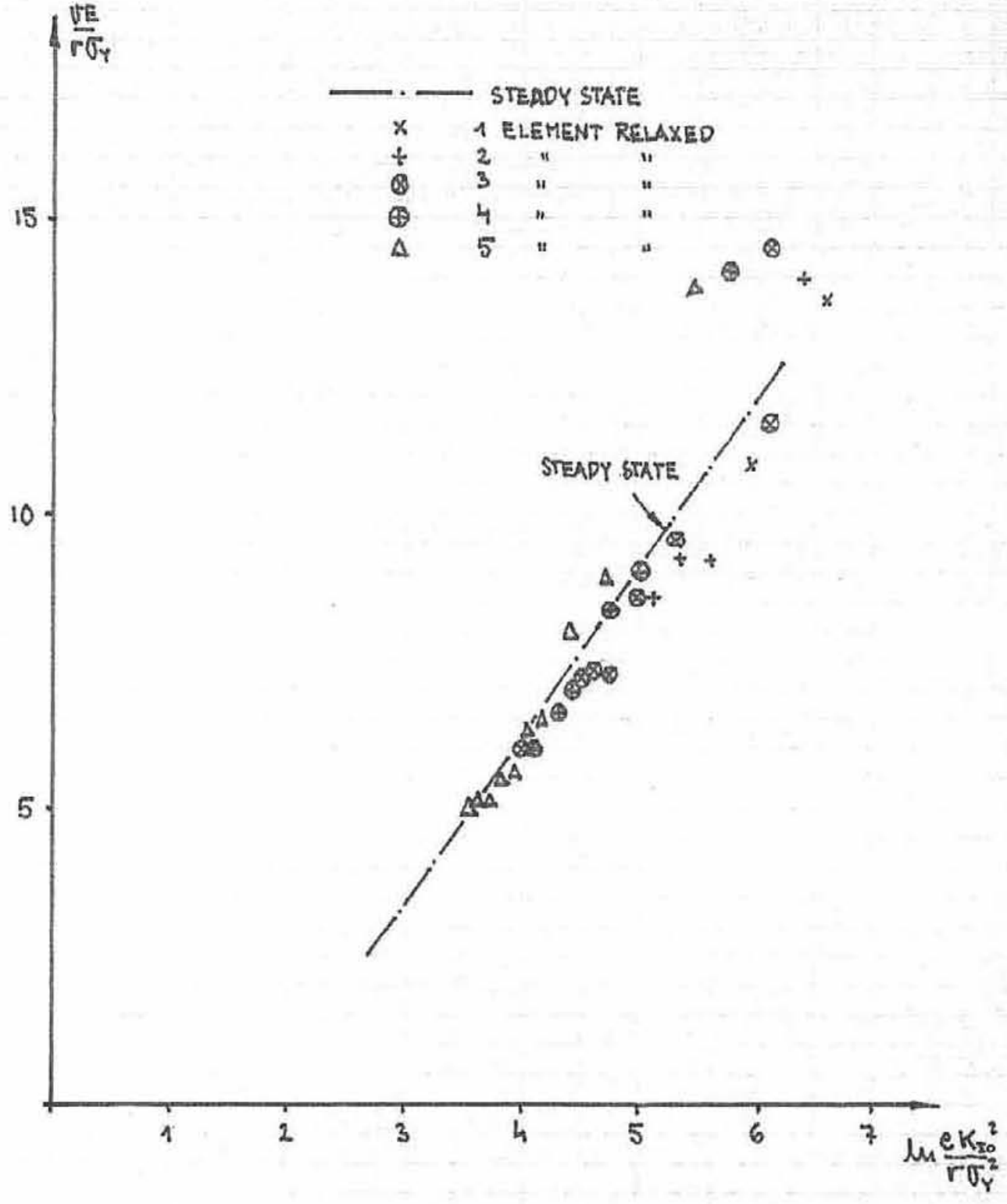

Fig. 23 Shape of the plastic zone for the situations in Fig. 21.

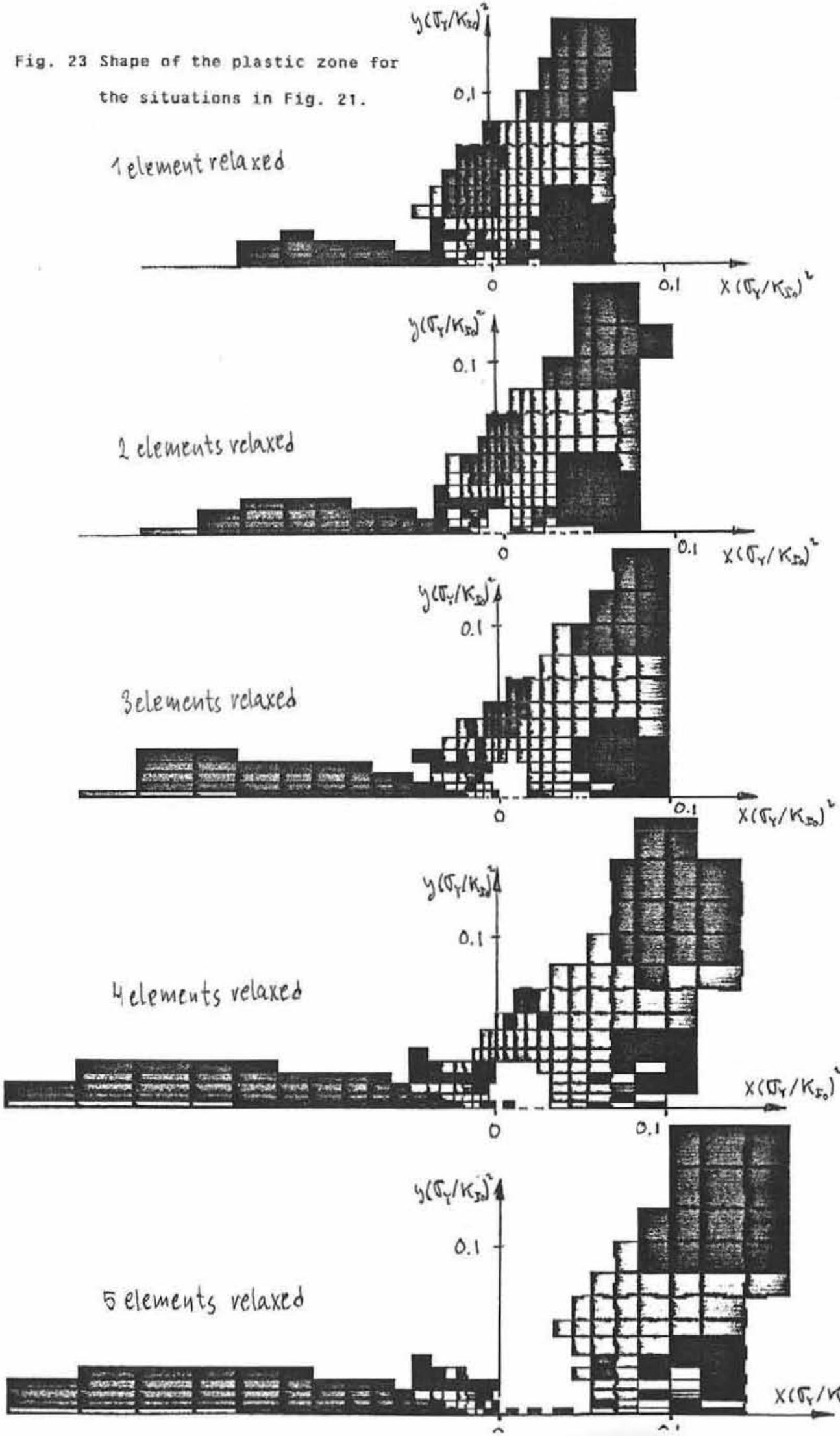

Fig. 24 Remote load K_I versus crack length and remote load K_I^E for the steady state case performing the identical near tip field versus crack length for a) unloading to $K_I = 0.6K_{Io}$, b) unloading to $K_I = 0$ and reloading to $K_I = 0.6K_{Io}$, c) unloading to $K_I = 0$ and reloading to $K_I = K_{Io}$ and d) no unloding and $K_I = K_{Io}$ during continued crack growth.